Table V—Norfloxacin in Plasma and Urine Following Single Oral Doses to an Individual

Dose, mg	Plasma Concentration, μg/mL Collection Time, h 0	0.5	1.0	1.5	2.0	3.0	4.0	6.0	8.0	12.0
200	0	0.63	1.22	0.81	0.60	0.28	0.47	0.33	0.21	0.14
400	0	0.51	1.42	1.21	0.91	0.74	0.52	0.42	0.28	0.22
800	0	2.91	3.22	2.43	2.20	1.88	1.31	0.83	0.73	0.41
1200	0	3.48	5.69	4.77	5.10	1.60	2.20	1.49	1.19	0.85
1600	0	0.73	2.73	4.61	5.15	4.61	3.54	2.26	1.63	1.13

Dose, mg	Urine Concentration[a] μg/mL Collection Interval, h 0–1	1–2	2–3	3–4	4–6	6–8	8–12	12–24	24–48
200	245	155	44	34	37	42	13	3	16
	(17.9)	(16.1)	(11.0)	(2.1)	(7.4)	(8.8)	(5.7)	(2.0)	(12.4)
400	271	69	41	129	102	109	32	6	4
	(14.4)	(35.9)	(16.8)	(9.8)	(11.6)	(10.0)	(14.4)	(1.1)	(3.0)
800	339	95	111	120	208	243	150	40	5
	(35.6)	(58.9)	(24.0)	(30.6)	(37.0)	(21.6)	(21.5)	(31.6)	(5.5)
1200	1125	1902	653	697	474	76	163	41	18
	(37.1)	(144.6)	(13.7)	(82.9)	(56.4)	(44.8)	(32.8)	(20.1)	(22.5)
1600	432	1414	505	161	524	583	134	70	10
	(34.6)	(60.8)	(72.2)	(67.6)	(74.4)	(43.1)	(56.3)	(39.9)	(30.4)

[a] Values in parentheses indicate total milligrams excreted.

standards. Representative standard curve data are shown in Table II. Reproducibility of this method was validated by the construction of calibration curves over the appropriate concentration ranges for plasma and urine analysis. The coefficients of variation so obtained are summarized in Tables III and IV. The day-to-day reproducibility of this method was demonstrated by assaying replicate aliquots of a spiked plasma sample. Thus, the interassay coefficient of variation was 8.7% (n = 8) for a 0.50-μg/mL plasma standard.

The assay method described in this report was used to quantitate norfloxacin levels in plasma and urine specimens from human subjects participating in an increasing-dose study of the drug. Representative data obtained for one of the volunteers is presented in Table V.

REFERENCES

(1) Y. Kumasaka, H. Nakahata, K. Imamura, and K. Takebe, *Chemotherapy*, **29(S-4)**, 56 (1981).

(2) K. Hirai, A. Ito, Y. Abe, S. Suzue, T. Irikura, M. Inoue, and S. Mitsuhashi, *Antimicrob. Agents Chemother.*, **19**, 188 (1981).

(3) T. Ozaki, H. Uchida, and T. Irikura, *Chemotherapy*, **29(S-4)**, 128 (1981).

(4) Y. Oomori, S. Murayama, Y. Abe, and T. Irikura, *Chemotherapy*, **29(S-4)**, 91 (1981).

(5) E. W. McChesney, E. J. Froelich, G. Y. Lesher, A. V. R. Crain, and D. Rosi, *Toxicol. Appl. Pharmacol.*, **6**, 292 (1964).

Application of Diffusion Theory to the Relationship Between Partition Coefficient and Biological Response

BRET BERNER ˣ and EUGENE R. COOPER

Received July 1, 1982, from *The Procter & Gamble Company, Miami Valley Laboratories, Cincinnati, OH 45247.* Accepted for publication December 14, 1982.

Abstract □ A diffusion model for transport through multilaminates is studied as a possible way to predict the optimal biological response of a set of congeners with respect to the oil–water partition coefficient, P. The model predicts the bilinear form typical of biological response data and, unlike the earlier kinetic model, also relates the results to physical processes, predicts the structure with the optimal response in terms of diffusion constants, and shows such an optimum prior to steady state for an infinite dose. Diffusion through an oil–water multilaminate causes extraordinary separation of permeating species based on partition coefficient and diffusion constant for times shorter than the lag time.

Keyphrases □ Multilaminates—oil–water, diffusion model, optimal biological response with respect to partition coefficient □ Partition coefficient—oil–water multilaminates, diffusion model, optimal biological response □ Optimal biological response—diffusion model, oil–water multilaminates, partition coefficient

In an earlier paper (1), we reviewed the kinetic (2) and equilibrium (3) models for predicting the optimal biological response of a set of congeners with respect to the partition coefficient, P. The kinetic models (1, 2) which treat this problem in terms of rate constants, can be a useful approximation for steady-state transport across a series of unstirred layers of the lipid–water interfaces. However, this kinetic model predicted a large degree of asymmetry (1) in the biological response curve with respect to P, and this asymmetry in transport is not satisfying from a fundamental physical viewpoint. Furthermore, the kinetic treatment neglects differences in diffusion between the lipid and aqueous phases. To understand the role of diffusion in transport across biological tissue of alternating physical properties, it is useful to apply classical diffusion theory to oil–water multilaminates.

Like the kinetic and equilibrium models, the diffusion model developed in this paper predicts a peak in the transport with respect to the partition coefficient for a multilaminated membrane. For a plot of the logarithm of

0022-3549/84/0100-0102$01.00/0

the concentration in the receptor compartment [log $C_R(t)$] *versus* log P, the diffusion model permits one to relate P_{max} (the partition coefficient which yields an optimal biological response) to the square root of the ratio of the diffusion constants in the water and oil phases. The initial and final slopes of such plots are equal to the number of oil laminates and water laminates, respectively. That is, non-steady-state permeation through multilaminates can produce an extraordinary separation of solutes with differing partition coefficients or diffusion constants. While this large separation factor is fascinating, it is atypical of biological response curves. To make the model more realistic, shunt pathways need to be introduced into the diffusion model.

Unlike the kinetic and equilibrium models, the diffusion model predicts a peak in the biological response with respect to P for both infinite and finite reservoirs (doses); the kinetic and equilibrium models predict an optimal biological response as a result of the depletion of the finite source (2). Provided water solubility is not the limiting factor, an infinite source reservoir may be used for biological response studies to determine whether equilibrium or nonequilibrium conditions prevail.

This paper presents the model for diffusion through multilaminates and relevant details of the finite difference method used to solve the equations. The theoretical transport curves obtained from this solution are also discussed. These results are then compared with the asymptotic solutions for times shorter than the lag time. [The details of the derivation of these asymptotic solutions and application to membrane separations are discussed elsewhere (4)]. The finite dose case is presented, and the time scale for diffusion is discussed.

THEORETICAL

An alternating series of n oil and $(n-1)$ water slabs (Fig. 1) separates a well-stirred water source compartment of initial solute concentration C_0 and a well-stirred water receptor compartment; the first oil membrane borders the source compartment. The variable to be solved for is $C_R(t)$, the concentration in the receptor compartment at time t, which is less than the characteristic time to reach equilibrium. This characteristic time is chosen to be the lag time for an identical membrane system with an infinite receptor compartment. The diffusing solute has an oil–water partition coefficient (P) and diffusion coefficients D_o and D_w in the oil and water phases, respectively. It is assumed that each barrier is uniform, and that solute equilibration at the interfaces is rapid compared with diffusion.

Within the ith membrane phase, the solute concentration, C_i, obeys Fick's law:

$$\frac{\partial C_i}{\partial t} = D_i \frac{\partial^2 C_i}{\partial x_i^2}, \qquad \text{(Eq. 1)}$$

where D_i equals D_o or D_w depending on the composition of that phase. At the interface, the following boundary conditions are satisfied:

$$D_i \left.\frac{\partial C_i}{\partial x_i}\right|_{\text{interface}} = D_i + 1 \left.\frac{\partial C_{i+1}}{\partial x_{i+1}}\right|_{\text{interface}} \qquad \text{(Eq. 2)}$$

and $C_{i+1} = \sigma C_i$ at the interface, where σ equals P or P^{-1} when the composition of the ith phase is water or oil, respectively. The initial conditions are:

$$C_1(x = 0, t = 0) = PC_o \text{ (water)} \qquad \text{(Eq. 3)}$$

and

$$C_i(x > 0, t = 0) = 0 \; (i = 1, 2, \ldots 2n-1),$$

where $x = 0$ denotes the interface of the source compartment and the first oil barrier. For these calculations the receptor compartment volume, V_R, was chosen to be 1 mL, the interfacial area to be 1 cm^2, and the source compartment volume, V_o, to be infinite or 1 mL. At the membrane–receptor interface, the boundary conditions are:

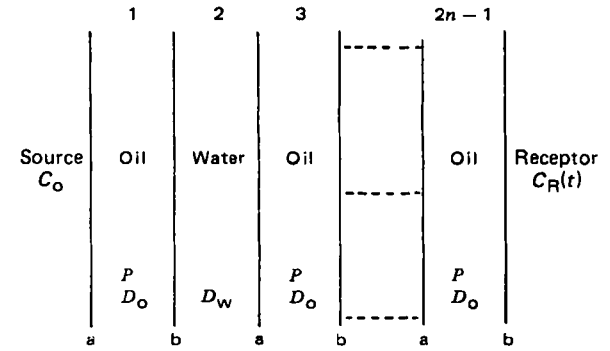

Figure 1—*The model for permeation through an oil–water multilaminate of* 2n − 1 *membranes.*

$$V_R \frac{\partial C_R}{\partial t} = -AD_o \frac{\partial C^b_{2n-1}}{\partial x_{2n-1}} \qquad \text{(Eq. 4)}$$

and $PC_R = C^b_{2n-1}$. The superscript b denotes the bth side of the $2n-1$ membrane. Analogous boundary conditions exist at the source–membrane interface for the finite source compartment case.

The method of finite differences (5) was used to solve Eq. 1 for $C_R(t)$. To obtain a stable numerical solution, the spatial and time increments, δx and δt, respectively, are selected subject to the condition (5):

$$\frac{D_i \delta t}{\delta x_i^2} = 0.5 \qquad \text{(Eq. 5)}$$

The important parameter to relate $C_R(t)$ to the biological response is C_0^{50}, the initial source concentration necessary to give 50% binding, A^{50}, at the receptor site at time t and partition coefficient P. Let there be a fixed, small volume fraction of lipophilic receptor binding sites in the receptor compartment; receptor binding is assumed to be rapid and, therefore, may be treated as an equilibrium process. C_0^{50} may be expressed as (1):

$$C_0^{50} = \frac{A^{50}}{aP^{\alpha}Q(t)} \qquad \text{(Eq. 6)}$$

where $Q(t) = C_R(t)/C_0$ and aP^{α} is the equilibrium constant for binding at the receptor sites. Since the details of the binding process are not known, it is appropriate to solve for $Q(t)$, which gives the main dependence of C_0^{50} on P for a given time. Note that throughout this paper $Q(t) = C_R(t)$.

Some of the parameters used in this model deserve comment. Although the volume ratio (oil–water) of 2:1 used in these calculations is not realistic for biological systems, calculations using a volume ratio of 1:10 showed no difference in any of the features discussed. It is not clear whether a constant total multilaminate thickness or a constant single membrane layer thickness as n varies is more appropriate for the modeling of biological response. There is no qualitative difference in the results of the two approaches, but t_L, the characteristic time for equilibration, for the latter is n^2 times t_l, for the former.

DISCUSSION

Diffusion Model Solution and Biological Response—To correlate the solution to the diffusion equation with biological response data, one needs to examine log $C_R(t)$ *versus* log P plots (Figs. 2 and 3). The bilinear function typical of biological response data (6) is in evidence for $n \geq 2$.

Even in the infinite source case shown (Figs. 2 and 3), the diffusion model predicts bilinear curves prior to establishing steady state. This is in contrast with the kinetic and equilibrium models, where this peaked function is due to the depletion of a finite dose reservoir. Since in the infinite source case the equilibrium model does not predict an optimal biological response, and the diffusion model does, an infinite dose biological experiment can be used to determine whether equilibrium or nonequilibrium processes prevail.

The shape of these bilinear curves is simply related to physical parameters in the diffusion model. The value of log P at which the peak in log $C_R(t)$ occurs (P_{max}) varies with the relative diffusion rate through each type of barrier (Fig. 2). In particular, it can be shown (4) that P_{max}

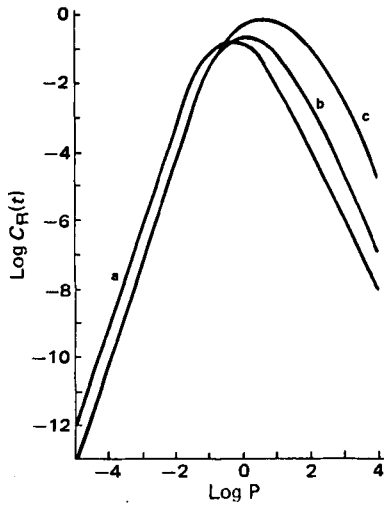

Figure 2—*Log* $C_R(t)$ versus *log P for* $D_o = 7 \times 10^{-5}$ *(a),* 7×10^{-6} *(b), and* 7×10^{-7} *(c)* cm^2/s, *where* D_w *is* 7×10^{-6} cm^2/s. *Note that the shift of the peak is proportional to* $(D_w/D_o)^{1/2}$, t = *1786, 7142, and 76,000 s, respectively, and* n = *3.*

is proportional to $(D_w/D_o)^{1/2}$. Provided the source is infinite, a knowledge of the solute diffusion constants in the two phases is sufficient to predict that structure of a homologous series which will give the optimal biological response. Since in biological systems $D_o < D_w$, the position of the peak must always be at log P >0.

While the position of the peak depends on the diffusion constants in the two phases, the initial and final slopes (Fig. 3) of a log $C_R(t)$ *versus* log P plot are n (the number of oil laminates) and $1 - n$ (the negative of the number of water laminates), respectively. For $0.1 < P < 10$, $C_R(t)$ is relatively insensitive to n. With increasing time, the peak becomes broader as does the range which is insensitive to n. Outside this range, however, there is exponential separation by the number of barriers based on partition coefficient; that is, $C_R(t)$ is proportional to P^n and $P^{(1-n)}$ for highly water- and oil-soluble solutes, respectively.

To relate these bilinear curves to a biological response, one recalls that biological response phenomena involve binding to lipophilic receptors, and therefore, the initial source concentration to give 50% binding is inversely proportional to $C_R(t)P^\alpha$ and not simply to $C_R(t)$ (Eq. 6). For a plot of log $C_R(t)P^\alpha$ *versus* P, a peak exists only when $n \geq 3$. The initial and final slopes of such plots are $(n + \alpha)$ and $(\alpha + 1 - n)$, respectively. P_{max} for a biological response is then approximately $[(D_w/D_o)^{1/2} + \alpha]$.

The slopes of these log $C_R(t)P^\alpha$ *versus* log P curves may be used to devise criteria for distinguishing which model best fits the data. To develop this criterion, α, which represents a difference in lipophilicity between the binding sites on the protein and the lipid phase, is approximated by one. Since $D_w/D_o > 100$, the optimal biological response occurs at a value of P > 10. At short times the initial slope predicted by both the diffusion and kinetic models is ≥2, whereas the initial slope predicted by the equilibrium model is 1 (1) (Table I). In marked contrast to the kinetic model, the final slope derived from diffusion theory need not be close to zero and, in fact, only equals 0 when $n = 2$ (Table I). Although measurement of the final slope is experimentally difficult, it is another method of distinguishing between the applicability of the diffusion model and other models. Note that for α exactly equal to one, only the diffusion model predicts an optimal biological response.

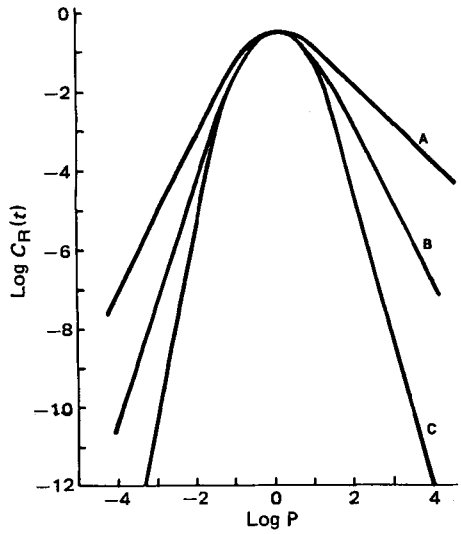

Figure 3—*Log* $C_R(t)$ versus *log P for* n = *2 (A), 3 (B), and 4 (C). The initial and final slopes are* n *and* −(n − *1), respectively;* t = *7142 s and* $D_w = 7 \times 10^{-6}$ cm^2/s.

Table I—Initial and Final Slopes for Models of Biological Response

Model	Initial Slope $P \ll 1$	Final Slope $P \gg 1$
Diffusion	$n + \alpha$	$\alpha + 1 - n$
Kinetic	$n + \alpha$	$\alpha - 1$
Equilibrium	α	$\alpha - 1$

While limited water solubility causes the final slopes of a biological response curve to be difficult to measure experimentally, the initial slope may be reasonably well determined. In an earlier paper, Kubinyi (6) fit a variety of biological data to the bilinear form:

$$\frac{bP^x}{(1 + \beta P)^y} \qquad \text{(Eq. 7)}$$

where x and y are adjustable parameters. Most of these data have initial slopes, $x \leq 1$. This result suggests that the equilibrium model is the best choice of operative process even though these data cannot be fit by the single adjustable parameter required in the equilibrium model. However, the initial slopes for the nonequilibrium model are time dependent and, at long times, may be closer to one.

Certain biological response data are probably governed by nonequilibrium transport phenomena, yet the data show $x \leq 1$. The proposed diffusion model may be inadequate due to neglect of certain physical processes. In particular, the inclusion of polar shunts through lipid membranes would shorten the equilibrium time for highly water-soluble permeating species. Consequently, the $P \ll 1$ regime might be best described by equilibrium or steady state, while the $P \gg 1$ region would be governed by non-steady-state phenomena. In this case, the initial slope of a log $P^\alpha C_R(t)$ *versus* P plot would be near unity. Inclusion of these shunts in the model creates a problem which is not easily solved and involves many adjustable parameters.

In summary, the advantages of the multilaminate diffusion model of biological response as compared to the kinetic model are (*a*) relating the results to physical processes, (*b*) the observation of a peak for an infinite dose in contrast to the other models, (*c*) the presence of a peak in log $P^\alpha C_R(t)$ *versus* log P, and (*d*) the existence of a simple asymptotic solution. However, as Hwang *et al.* (7) and Yalkowsky and Flynn (8) have shown for intestinal and vaginal absorption, a multilaminate model may not be appropriate for tissues in general, since aqueous pores may be present in the tissue.

Comparison with the Asymptotic Solutions for Short Times—Using a simple approximation, one can derive the asymptotic solutions for short times and P very different from unity (4). To understand the extreme separation predicted by this theory, it is useful to compare the finite-difference results with the asymptotic solutions.

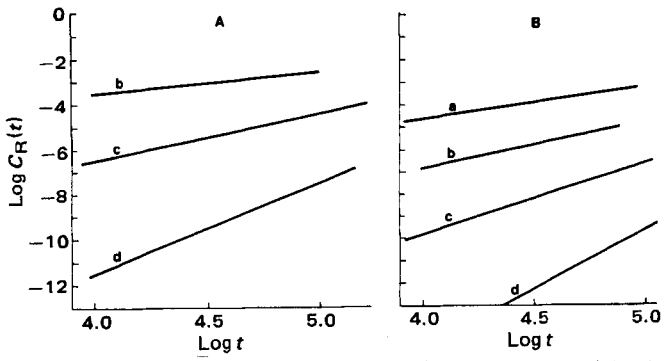

Figure 4—*Log* $C_R(t)$ versus *log* t *for* $P = 10^4$ *(A) and* $P = 10^{-4}$ *(B) for* n = *1 (a), 2 (b), 3 (c), and 4 (d). Note that the plots are linear with slopes of* n − *1 and* n *for* $P = 10^4$ *and* 10^{-4}, *respectively.*

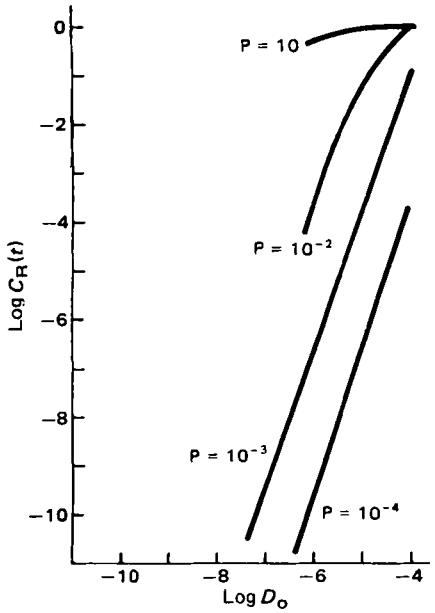

Figure 5—*Log* $C_R(t)$ versus *log* D_o *for several P. For* $P \ll 1$, *the plots are linear with a slope of 3 since* n = 3. *For larger P, log* $C_R(t)$ *is increasingly independent of* D_o; t = 71,390 *s.*

At short times ($t < t_L$) it may be shown that $P \ll P_{max}$:

$$C_R(t) \approx \frac{Al_w}{V_R n!}\left(\frac{D_o P t}{l_o l_w}\right)^n C_0 \qquad \text{(Eq. 8)}$$

and for $P \gg P_{max}$:

$$C_R(t) \approx \left(\frac{D_w t}{P l_o l_w}\right)^{n-1} \frac{C_0}{(n-1)!} \qquad \text{(Eq. 9)}$$

where t_L is the lag time (9) and l_o and l_w are the thickness of a single oil and water membrane, respectively. To demonstrate the validity of these equations, one examines the values of $C_R(t)$ obtained by the finite-difference method. If $t < t_L$ and $P \ll 1$, log $C_R(t)$ should be a linear function of log P, $-\log D_w$, $-\log t$, $\log l_o$, and l_w with a slope equal to the number of water barriers. Figure 4 is a plot of log $C_R(t)$ *versus* log t for several n. In Figs. 5 and 6 we plotted log $C_R(t)$ *versus* log D_o and log D_w, respec- of water barriers. Figure 4 is a plot of log $C_R(t)$ versus log t for several n. In Figs. 5 and 6 we plotted log $C_R(t)$ *versus* log D_o and log D_w, respectively, for various P; the separation of solutes at different diffusion constants is enormous. The predicted linear dependence and slopes stated in Eqs. 8 and 9 are all verified in these three figures. More important for the understanding of optimal biological response, log $C_R(t)$ should be a linear function of log P in the small and large P limits.

Permeation from a Finite Source—The effect of a finite source as a function of time is shown in Fig. 7. At short times, the curve is identical to the infinite source case. As t becomes longer the curve broadens and

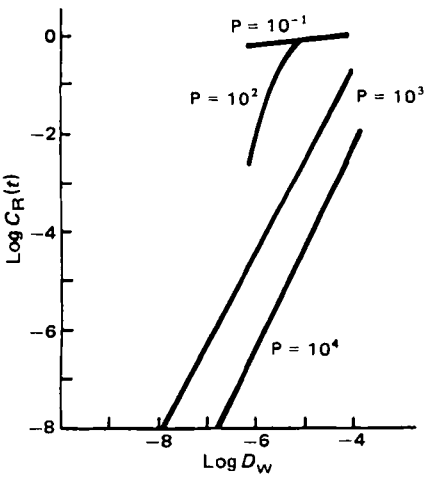

Figure 6—*Log* $C_R(t)$ versus *log* D_w *for several P. For* $P \gg 1$, *the plots are linear with a slope of 2 since* n = 3. *For smaller P, log* $C_R(t)$ *is increasingly independent of* D_w; t = 71,390 *s.*

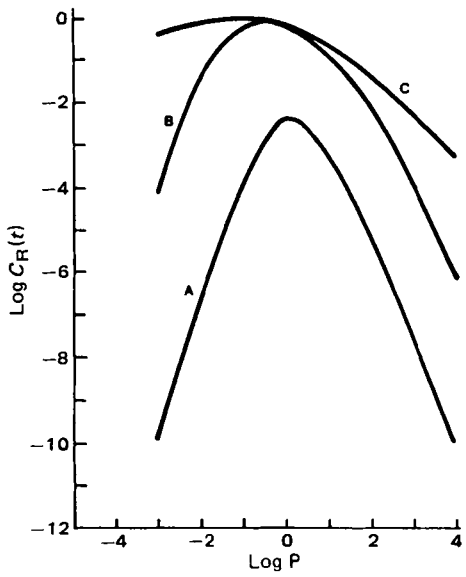

Figure 7- *Log* $C_R(t)$ versus *log P for* t = 1.786×10^3 *(A),* 7.829×10^4 *(B), and* 4.0×10^6 *s, with a finite source reservoir,* V_o = 1 *mL,* n = 3. *Note the shift of the peak and the flattening of the curve with increasing time.*

the peak shifts in the negative log P direction; at infinite time (the equilibrium case) the initial slope of a log $C_R(t)$ *versus* log P plot is zero, and the final slope is −1. According to the oil–water diffusion model, the peak in log $C_R(t)$ with respect to log P can occur at values of $P < 1$ only if there is a finite dose. Thus, with an infinite source, $P_{max} < 1$ should not occur unless water solubility is limiting. With a finite reservoir, such a peak position may result from either equilibrium or nonequilibrium processes.

Time Scale for Diffusion—It is useful to study the solution to Eq. 1 for the given initial and boundary condition in two limits: the long-time or equilibrium limit and the short-time nonequilibrium limit. A characteristic time which serves as an upper bound to the validity of the solution for short times needs to be defined; the diffusional lag time, t_L, is a lower limit to this characteristic time. For a large number of membrane pairs, $n^2 \gg 1$, t_L is given by (9):

$$t_L = \frac{V_o D_w + P V_w D_o}{6 D_o D_w}\left(V_o + \frac{V_w}{P}\right) l^2 \qquad \text{(Eq. 10)}$$

where l is the total thickness of the composite of slabs, and V_o and V_w are the volume fractions of oil and water, respectively. For *in vitro* experiments involving individual cells, t_L for distances equal to cell diameters is of the order of seconds, and the equilibrium model should be utilized in the interpretation of such biological response data. On the other hand, for *in vitro* or *in vivo* experiments involving diffusion through tissue, t_L for $l > 10$ μm can range from the order of hours to months for P very different from unity; consequently, the nonequilibrium model might be applicable for many experiments.

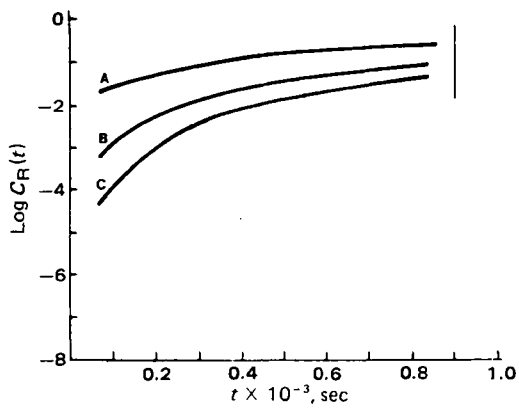

Figure 8—*Log* $C_R(t)$ versus t *for* $P = 10^{-2}$ *for* n = 1 *(A), 2 (B), and 3 (C) membranes. The lag time (perpendicular line) is shown as an estimate of the time of convergence of the curves for different* n.

The existence of aqueous shunts in the oil phase may shorten t_L drastically. To examine the validity of t_L as a characteristic time, one plots $C_R(t)$ against t for several values of n for an infinite source (Fig. 8). At long times, $C_R(t)$ asymptotically approaches the equilibrium solution, which for an infinite source is:

$$\lim_{t \to \infty} C_R(t) = C_0 \qquad \text{(Eq. 11)}$$

As shown in Fig. 8, the lag time, t_L, is a reasonable estimate of the time of convergence of the curves for different n.

REFERENCES

(1) E. R. Cooper, B. Berner, and R. Bruce, *J. Pharm. Sci.*, **70**, 57 (1981).

(2) J. T. Penniston, L. Beckett, D. L. Bentley, and C. Hansch, *Mol. Pharmacol.*, **5**, 333 (1969).

(3) T. Higuchi and S. S. Davis, *J. Pharm. Sci.*, **59**, 1376 (1970).

(4) B. Berner and E. R. Cooper, *J. Memb. Sci.*, **14**, 139 (1983).

(5) J. Crank, "The Mathematics of Diffusion," Oxford University Press, London, 1975.

(6) H. Kubinyi, *J. Med. Chem.*, **20**, 625 (1977).

(7) S. Hwang, E. Owada, T. Yotsuyanagi, L. Suhardja, N. F. H. Ho, G. L. Flynn, and W. I. Higuchi, *J. Pharm. Sci.*, **65**, 1576 (1976).

(8) S. H. Yalkowsky and G. L. Flynn, *J. Pharm. Sci.*, **62**, 210 (1973).

(9) R. M. Barrer, in "Diffusion in Polymers," J. Crank and G. S. Park, Eds., Academic, New York, N.Y., 1968.

Synthesis and Anticonvulsant Properties of Some 2-Aminoethanesulfonic Acid (Taurine) Derivatives

LARS ANDERSEN *, LARS-OLAV SUNDMAN *x, INGE-BRITT LINDÉN *, PIRJO KONTRO ‡, and SIMO S. OJA ‡

Received March 1, 1982, from the **Research Laboratories of Medica Pharmaceutical Company, Ltd., Box 325, SF-00101 Helsinki 10*, and ‡*Department of Biomedical Sciences, University of Tampere, Box 607, SF-33101 Tampere 10, Finland.* Accepted for publication September 2, 1982.

Abstract □ A series of 2-acylaminoethanesulfonamides were synthesized by treating the corresponding sulfonyl chlorides with ammonia, a primary, or a secondary amine. A few compounds displayed marked anticonvulsant activity in mice when tested for their potency in the maximal electroshock seizure test. The piperidino, benzamido, phthalimido, and phenylsuccinylimido derivatives were active, whereas the succinylimido, saccharinylimido, and norbornendicarboxylimido compounds showed no activity. The interference with the sodium-independent taurine binding to mouse brain synaptic membranes was assessed to elucidate the possible mode of anticonvulsant action.

Keyphrases □ Anticonvulsant agents—potential, 2-aminoethanesulfonic acid (taurine) derivatives, synthesis □ Synthesis—2-aminoethanesulfonic acid (taurine) derivatives, anticonvulsant activity in mice □ Taurine—synthesis of derivatives, anticonvulsant activity in mice

Taurine, 2-aminoethanesulfonic acid, is abundant in excitable mammalian tissues such as the brain, sensory organs, heart, and other muscles (1). In these tissues taurine has recently been considered an essential effector in the regulation of neuronal communication, possibly as an inhibitory synaptic transmitter, neuromodulator, or stabilizer of excitable membranes (2, 3). Taurine effectively prevents seizures when administered intracerebroventricularly to an animal model, but clinical trials with epileptic patients using oral or intravenous administration have been only partially successful (4).

Taurine is quite polar, and its penetration from plasma into brain tissue is apparently hampered by its hydrophilic properties (5). We have attempted to prepare more lipophilic derivatives of taurine which would still possess an inhibitory action at central synapses. Lipophilization of taurine was effected by both acylation and conversion of the sulfonic acid group to various amides. In this way the shape of the molecule and the intramolecular electron distribution, both of which may be essential for the taurine-like inhibitory action (6), were expected to be unchanged. It is also significant that sulfonamides are generally atoxic.

RESULTS AND DISCUSSION

The compounds studied are of the general structures A and B (see Table I for R_1 and R_2 designations).

$R_1CH_2CH_2SO_2NH_2$ (A) $\qquad$ $R_1CH_2CH_2SO_2R_2$ (B)

Although several earlier reports (7–10) have described similar compounds, these studies evaluated the compounds for antibacterial and antimalarial activity. They were either inactive or only slightly active in this respect.

Compounds II, IVa–g, V, and VIIIa–b inhibited maximal electroshock (MES)-induced convulsions in mice (Table II). The most potent compounds were II, IVc, IVd, IVe, IVg, and V, which had ED_{50} values ≤100 mg/kg. It was found that the sodium-independent binding of [^{3}H]taurine to isolated synaptic membranes was inhibited by III, IVa, V, and VIc. In general, no parallelism was observed between anticonvulsant action and inhibition of taurine binding. Only V may act by interfering with the attachment of taurine to its membrane binding sites.

The acyltaurinamides and *N*-substituted acyltaurinamides were synthesized from the corresponding sulfonyl chlorides and ammonia, a primary, or a secondary amine as described previously (7–9, 11). These compounds are colorless, crystalline substances with a somewhat bitter taste. They are insoluble or slightly soluble in water, but soluble in polar organic solvents.

EXPERIMENTAL[1]

***N*-[2-[(Methylamino)sulfonyl]ethyl]benzamide (IVb), *N*-[2-[(Ethylamino)sulfonyl]ethyl]benzamide (IVc), *N*-[2-[(Dimethylamino)sulfonyl]ethyl]benzamide (IVd), *N*-[2-[[(1-Methylethyl)amino]sulfonyl]ethyl]benzamide (IVe), *N*-[2-[(Butylamino)sulfonyl]ethyl]benzamide (IVf), and *N*-[2-[[(1,1-Dimethylethyl)amino]sulfonyl]ethyl]benzamide (IVg)**—These compounds were prepared as described below for IVg. To *tert*-butylamine (10.92 g, 0.150 mol) was added with cooling and stirring (ice-bath) the substituted sulfonyl chloride (7.66 g, 0.031 mol) over a 25-min period. After 20 min stirring additional *tert*-butylamine (3.64 g, 0.05 mol) was added, and the stirring was continued at room temperature. Water (75 mL) was added, and the excess amine was removed with a stream of air. The precipitate was re-

[1] Melting points were determined in open capillary tubes and are uncorrected. Elemental analyses were performed by Janssen Pharmaceutica NV, Analytical Department, Beerse, Belgium. NMR data were recorded on a JEOL FX-60 spectrophotometer.

0022-3549/84/0100-0106$01.00/0